The Kinetics of Natural Ageing in 6000 Alloys - a Multi-method Approach

J. Banhart[1,3], C.S.T. Chang[1] , Z. Liang[1], N. Wanderka[1], M.D.H Lay[2] and A.J. Hill[2]

[1] Helmholtz-Centre Berlin for Materials and Energy, Hahn-Meitner-Platz, 14109 Berlin, Germany

[2] Materials Science and Engineering, CSIRO, Normanby Rd., Clayton, VIC 3168, Australia

[3] Technische Universität, Institute of Materials Science, Hardenbergstr. 36, 10623 Berlin, Germany

Room temperature 'natural' ageing in Al-Mg-Si alloys was studied by means of six different techniques: electrical resistivity, thermoanalysis, hardness measurement, lifetime of positrons, 3D atom probe and small-angle neutron scattering in order to identify different clustering stages and to study when the negative effect of natural ageing on subsequent 'artificial' ageing sets in. The various measurements show that natural ageing is much more complex than anticipated and at least four different stages can be distinguished.

1. Introduction

Al-Mg-Si alloys can be hardened by 'artificial' ageing – i.e. by baking the solutionised and quenched solid solution at 150°C to 180°C. Such '6000 series' alloys are now widely used versatile materials due to their potential to be aged to medium strength while having good metal forming properties in the non-aged state. In addition, corrosion and welding properties are reasonable, costs are moderate and handling is simple. They have found many applications in the transport industry (automotive, railway), architecture and consumer goods industry. One of the peculiarities of Al-Mg-Si alloys, the adverse effect of room temperature 'natural' ageing on a subsequent artificial ageing step, has been known for a long time, but still the exact reasons for this effect are being investigated. Natural ageing (*NA*) is technologically of little relevance for 6000 series alloys because these are more efficiently aged artificially (*AA*). Because NA that occurs during processing can have a 'negative' effect on AA, it is worthy of detailed study. Of all the imaging techniques, only 3D atom probe can resolve the clusters formed during NA, but indirect techniques such as thermal analysis, resistivity measurement, X-ray scattering, and positron annihilation spectroscopy can be utilised to build a comprehensive picture of phase evolution. Experience shows that one such indirect technique is not powerful enough to reveal the subtle changes in a quenched alloy during NA and that many of these methods have to be applied. Extracting and comparing information from the literature is difficult due to the use of too many different alloys and ageing conditions. This complexity is why an effort has been started to do such analyses on a few pure ternary alloys while keeping the variety of heat treatments to a minimum.

2. Available methods and the "6000 alloy problem"

The study of 6000 series alloys is complicated by their very low Mg and Si content, i.e. ≤1.5% Si or ≤1.2 wt.% Mg. This implies that any element-sensitive probe will yield a low signal-to-noise ratio (SNR). As Mg, Al and Si are neighbouring elements in the periodic table and the interaction of X-rays and electrons scales with the electron density, element contrast is low in electron microscopy and X-rays are diffracted from the different atoms in a similar way. X-ray small-angle scattering (SAXS) suffers from the very small scattering-length density difference between the precipitates and the matrix. Unfortunately, small-angle neutron scattering (SANS) has to deal with a similar problem since the scattering lengths of the three elements are quite similar.

Transmission electron microscopy (TEM) and 3D atom probe (3DAP) have been applied to 6000 alloys, but only 3DAP reveals the size and composition of clusters formed during NA [1,2]. Of the

available methods probing atomic environments, *positron lifetime spectroscopy* (PALS) has been found to be sensitive enough to detect clustering phenomena in such alloys [3,4,5].

Small-angle X-ray scattering (SAXS) suffers from the poor SNR in 6000 alloys, with a slight advantage for *small-angle neutron scattering* (SANS). *Differential thermal analysis* (DSC) has been used by many groups to elucidate the cluster formation process during NA of 6000 alloys, e.g. [6]. It provides averages of the heat evolution caused by the formation of all clusters in the sample. *Electrical resistivity* is extremely sensitive to very small changes of the atom configuration induced by atomic diffusion and has been often used to characterise NA in Al-Mg-Si alloys, e.g. [5,7]. *Mechanical properties*, e.g. hardness or tensile strength, can be easily measured in various stages of NA and reflect the resistance to dislocation movement built up by clusters and emerging precipitates.

3. Sample preparation

Two alloys of the Al-Mg-Si system were studied: one with a low content in both Si and Mg (denoted 'H'), one with a higher one (denoted 'F'). Past research has revealed that H does not show the negative effect while F does [8]. The alloys were prepared by Hydro Aluminium (Bonn) from very pure elements. The final product came as a rolled sheet of 1 mm thickness and was chemically analysed by sparc-induced optical emission spectroscopy (OEM) after manufacture.

Table 1. Alloy compositions as determined by OES (Optical Emission Spectroscopy)

alloy code	Mg[a]	Si[a]	Fe[b]	Mn[b]	Cu[b]	Cr[b]	Bi[b]	Sn[b]	others[b,c]	commercial equivalent
H	0.40	0.40	<5	<2	<2	<2	<10	<10	<5	6060
F	0.59	0.82	<5	<2	<2	<2	<10	<10	<5	6111, 6082

[a] in % by mass; [b] in ppm by mass; [c] Ni, Zn, Ti, B, Be, Ca, Cd, Co, Ga, In, Li, Na, P, Pb, Sb were analysed

Solution heat treatment was carried out at 535°C to 540°C for typically 30 min or 60 min in air, after which the samples were quenched into ice water. For studies of NA, the samples were further processed very fast so that the first hardness, resistivity or positron lifetime data could be obtained with as little delay as possible, typically <2 min (see results section). For the electrical resistivity measurement, the sheets were drawn to wires of 0.8 mm thickness.

4. Experimental studies using different techniques

Throughout this chapter we will use the term 'natural ageing' (NA) for any ageing at 'room temperature' ranging from 18°C to 22°C here. Artificial ageing (AA) was carried out at 180°C. If NA was performed before AA, we call it 'natural pre-ageing' (NPA), if it was carried out after AA, the term 'natural secondary ageing' (NSA) is used. We first present studies of simple NA at constant 'room temperature' directly after quenching. NA in combination with AA will be presented in 4.2.

4.1 Natural ageing (NA)

Hardness: Figure 1 shows that the hardness for alloy F initially increases much faster than that of alloy H and that different stages can be distinguished for alloy F. The density of the data points does not allow us to decide clearly whether there are 2 or 3 different stages. One interpretation (marked '1') involves a stage of fast initial hardening up to 85 (+30,20) min, after which hardening slows down and the further course becomes approximately parallel to that of alloy H. Hardness as a function of log(t) shows approximately linear slopes. The other interpretation (marked '2') implies an intermediate hardening range from 50±10 min to about 800±200 min after quenching for alloy F.

The data shown for t > 60 min is compatible with that given in the literature [7] where, however, the change from rapid hardening to slow hardening rate cannot be seen since the measurements start after 60 min. The very fast ageing rate in our alloy F can be explained by the purity of the metals used,

since some additional elements are known to slow down natural ageing, probably due to trapping of vacancies after quenching, which are then no longer available to mediate the early clustering process.
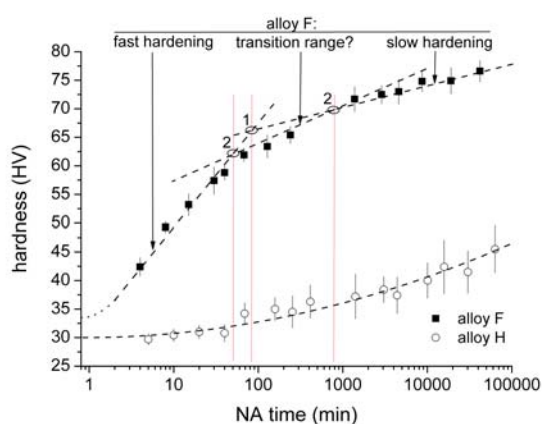
Figure 1. Hardness evolution of alloys H and F during NA at 20°C after solutionising and quenching (10 points each). The vertical dotted lines separate ranges in which the logarithmic increase for alloy F follows straight lines of distinct slopes. The labels '1' and '2' denote the times of crossover between different slopes, assuming either two or three different regimes. Broken lines are best fits [13].
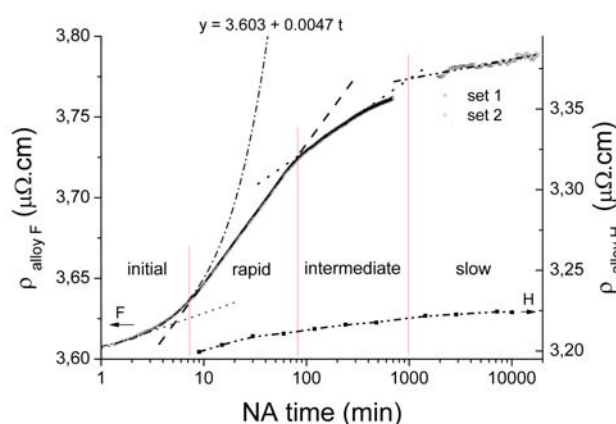
Figure 2. Electrical resistivity of alloys H and F during natural ageing at 21°C after solutionising and quenching. The broken lines indicate ranges where the resistivity increases as log(t), which is disputable for the initial stage. The dash-dotted line is a linear fit to the resistivity data up to 10 min (appearing as an exponential in this representation). Data for alloy H measured with a lower time resolution is displayed for matters of comparison [13].

NA in Al-Mg-Si alloys has been discussed such that it is initially silicon that dominates cluster formation due to its higher diffusivity and lower solubility in aluminium and that in a later stage magnesium starts contributing to cluster formation [6]. Although this picture is directly supported only by data about chemical changes within precipitates formed at higher temperatures, it is commonly assumed to be valid at room temperature too. Accepting this assumption, initial clustering would lead to Si-rich clusters which increase hardness at a fast rate. Later, i.e. after ~50 minutes, some fraction of these would begin to enrich in Mg and cause further hardening (50 min – 800 min), but at a lower rate, until finally all clusters are enriched with Mg and further cluster growth is dominated by Mg diffusion (the slow rate process for times >800 min). This slow process has been tentatively attributed, in alloy F, to the diffusion of Mg to Si-Mg co-clusters. The lack of a fast process in alloy H is likely due to the much lower percentage of Si in alloy H (50% less than in alloy F). However, direct proof for this picture is lacking at this point of the discussion.

Electrical resistivity: Figure 2 shows that the resistivity increases at any instant, and that again distinct stages can be distinguished by their slopes that appear linear if the time is used on a logarithmic scale. We observe an initially fast increase of resistivity. After about 85±15 min, the slope changes to a lower value within roughly 30 min and the resistivity continues to increase up to the end of the period investigated. Possibly, another change in slope after about 1000±300 min can be detected. Obviously, all the changes are much smaller in alloy H than in alloy F. These findings are in good agreement both with in-situ measurements reported in the literature [9] and with recent measurements [5] where very similar alloys were investigated ex-situ, i.e. the measurements were carried out at 77 K temperature and the sample was allowed to anneal at room temperature between two measurements. As for hardness, there is an initial fast reaction that changes into a slower one after 85 min which is very similar to the time the hardness course changes its slope. It is reasonable to assume that the same change of the rate of cluster growth or cluster composition postulated as a reason for the change of hardness, influences resistivity as well. More specifically, it is assumed that

in the regime of fast increase the diffusion of solute atoms is easy since enough vacancies are available for solute transport. Although vacancies do form vacancy/solute complexes, such pairs could break up and allow diffusion of other solute atoms, especially silicon. In the later stage, the vacancies are postulated to become increasingly trapped in larger solute/vacancy complexes also containing magnesium, and diffusion slows down [10]. In summary, alloy F shows similar stages in hardness and resistivity that relate to cluster formation and growth and solute diffusion. The fast process (at shorter times up to ~50 or 85 minutes) is attributed to Si diffusion dominated cluster formation and growth and the slower process is attributed to Mg diffusion dominated co-cluster growth.
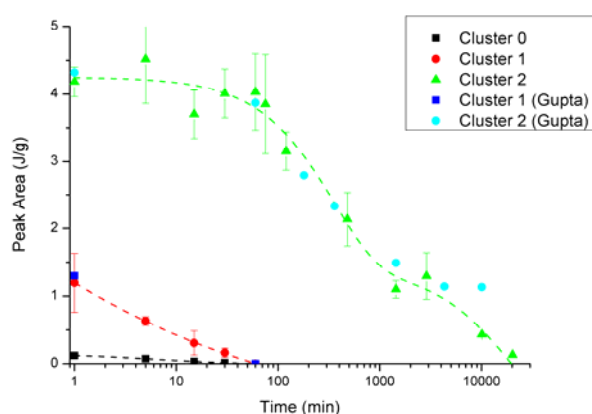
Figure 3. Change of DSC peak area of the 3 clustering reactions detected as a function of natural pre-ageing (22°C) time [11]. Values for a similar alloy included [6].
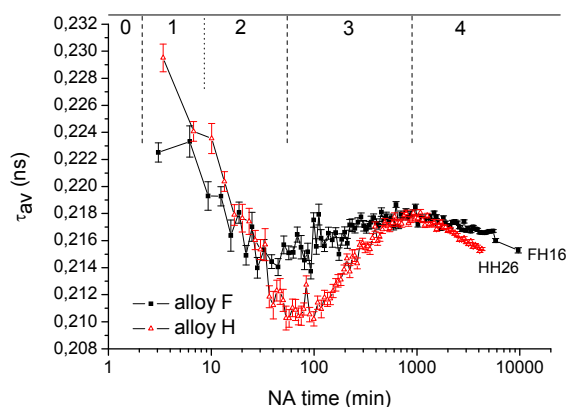
Figure 4. Average positron lifetime for alloy H and F samples measured directly after solutionising and quenching. Experimental details, see [12].

Differential thermo-analysis: DSC was carried out on samples of alloy F using a Perkin and Elmer 'Pyris 6' differential scanning calorimeter. Alloy F specimen were inserted into the DSC apparatus within 1 min after quenching and measuring with 10 K/min heating rate, as well as other samples which were left to pre-age at room temperature for up to 20,000 min (1 weeks) before [11]. In the temperature range −50°C to 150°C, three exothermal clustering reactions could be detected. These reactions could be decomposed into various Gaussians, the area of which is shown in Figure 3. The formation of the two initial clusters is coordinated and completed after 60 min, whereas the third exothermic peak moves to higher temperatures and reduces in magnitude with NPS times up to 20,000 min. Others have observed these features in DSC studies of 6000 series alloys and have attributed the ~50°C reaction to mainly Si clustering and the ~80°C to 120°C reaction to clustering reactions in which Mg is added [6].

Positron annihilation lifetime spectroscopy (PALS): The average positron lifetime was measured at 18°C as a function of time directly after quenching into ice water. Figure 4 shows the course for an alloy H and F. We observe up to four distinct stages: in alloy F (but not in H) a short period (7 min to 10 min) of constant (or even very slightly increasing) lifetime of 0.222 to 0.227 ns, then a period of lifetime decrease up to t≈60 min for alloy F (continuous decrease up to t≈80 min for alloy H), reaching 0.213 ns (0.210 ns), after which the lifetime increases again for typically 800 min to 1000 min, reaching 0.217 ns. This increase then reverses into another decrease which continues for longer than 10,000 min and approaches the lifetime (≈0.213 ns) measured in the as-received alloys. The interpretation of this very unusual behaviour is not straight-forward and in parts still speculative. Immediately after quenching there is a large density, i.e. 10^{-3} to 10^{-2} at.%, of free non-equilibrium vacancies in the alloy. Unlike pure metals where these vacancies gradually annihilate at grain boundaries, dislocation loops or the sample surface, in our alloys, containing typically 1% solute
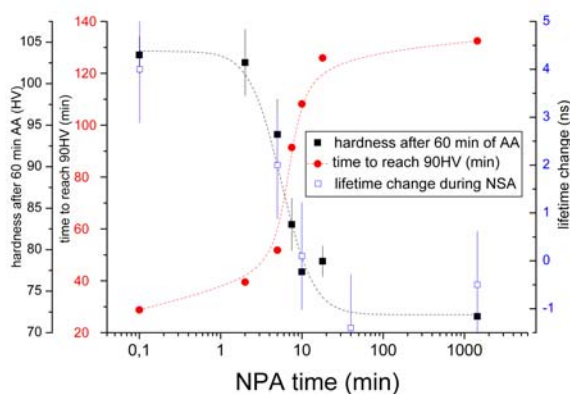
Figure 5. Display of different quantities after a given NPA time: hardness reached after 60 min of AA, time to reach a hardness level of 90HV and change in positron lifetime during secondary ageing. Note that the value for 'no NPA' is set to 0.1 min to allow for display on the logarithmic scale which is a realistic but not an exactly measured delay time. A critical change occurs from >2 min to 18 min of NPA at 'room temperature' and this critical change is defined as the negative effect [13].

atoms such as Mg and Si, vacancy-solute complexes are formed very quickly, long before we can measure the first positron lifetime (which is approximately 2–3 min following quench). The initial lifetimes measured (0.220 ns to 0.230 ns) therefore express the lifetime of such complexes and not that of free vacancies in Al which is ≈0.250 ns. The stage of lifetime decrease in a period up to ~60–80 min coincides with characteristic times found using DSC, resistivity and hardness measurement. Accepting the assumption that silicon clustering occurs first, these clusters could be responsible for the initial decrease in positron lifetimes by 0.010 to 0.020 ns. The ensuing lifetime increase after 60-80 min would then correspond to the addition of Mg to existing Si-clusters (co-clustering) or the formation of new Mg-rich clusters. As this increase is not observed for an alloy very low in Mg [12], this explanation appears very plausible. The final decrease after about 800 min after quenching might be caused by ordering phenomena within the clusters and that vacancies that were previously trapped in the clusters are finally released and diffuse to sinks.

3D atom probe and small-angle neutron scattering: Both methods applied to samples aged at 'room temperature' for a long time (»1 day) reveal signs of cluster formation, but the time resolution is far too low to allow us to study the different stages indicated by the other methods presented here. Therefore we refer to Ref. 13 for further details.

4.2 Artificial ageing (AA) after natural pre-ageing (NPA)

We now discuss some of the phenomena occurring during NA by studying their impact on a subsequent AA step.

Hardness: The hardness evolution of alloy F during AA at 180°C was measured for different natural pre-ageing (NPA) times at 'room temperature' after quenching but before AA. The main observation is that NPA has an adverse effect on hardness evolution during AA, the so-called 'negative' effect reported many times in the literature, e.g. [14]. We observe that both the rate of initial hardening is reduced and the final peak hardness drops from 120 to 110 HV [13]. What is unusual is that the negative effect is observed already for very short NPA times. Even after 2 min the initial slope starts to reduce, for 5 min, 7.5 min and 10 min the effect gets stronger and for 18 min of NPA the hardening course is very close to the course observed for 10,000 min of NPA. Figure 5 expresses this observation by showing two different measures for the negative effect, namely hardness after 60 min of AA and the time needed to reach 90 HV hardness value. Both measures for the loss of AA hardenability express the same behaviour. Moreover, the observed changes in the positron lifetime change during secondary ageing – discussed in the next section – correspond well with the loss in hardness response. This provides a hint that there is a common reason for these findings.

Positron annihilation lifetime spectroscopy (PALS): In order to characterise the effect of NPA prior to AA, a so-called secondary ageing experiment was carried out. In this type of experiment,

samples are artificially aged for a very short time (here 1 min) in an oil bath at 180°C. After removal from the oil bath, cooling and drying, a PALS measurement is carried out for typically 1000–5000 min (≈1–4 days) at 18°C. It is known from the literature that natural secondary ageing (NSA) even after some AA can take place in 6000 alloys and can influence the positron lifetime [3]. As Figure 6 shows, 1 min of ageing at 180°C has a huge impact on lifetime which is reduced from 0.223 ns after quenching, see Figure 4, to about 0.210 ns.
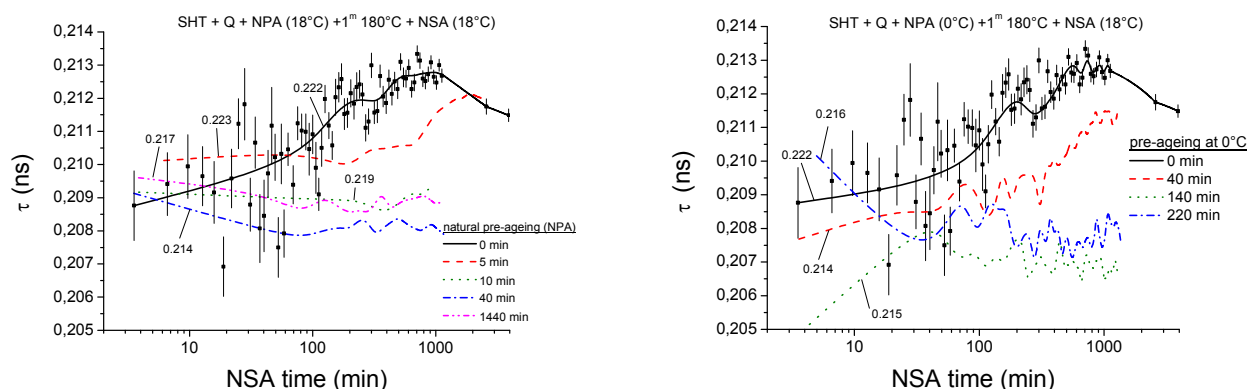
Figure 6. (a) Positron lifetimes in alloy F during natural secondary ageing at 18°C (NSA) after NPA at 18°C and AA for 1 min at 180°C. Individual data points are shown for one of the curve [13]. (b) same as (a) but NPA at 0°C. The lifetimes immediately before AA are given for each curve (marked by short dashes).

This decrease during AA is not easy to explain, unlike its analogy in Al-Cu alloys [15]. Two explanations seem possible: one could assume that vacancies embedded in clusters containing Si and/or Mg annihilate positrons more efficiently than anticipated from extrapolations based on pure elements values. Mg and Si are both elements with a higher atomic volume (23.3 and 20 $Å^3$/atom) than Al (16 $Å^3$/atom) and if Mg and Si were compressed into the denser fcc lattice of Al, their electronic density could increase so much that the lower lifetimes become explicable. Another explanation is to assume that after AA clusters are formed in the supersaturated matrix in such a low density that the surrounding solute and vacancy-depleted bulk would contribute to positron annihilation with the typical lifetime component around 0.160 ns. However, a two-component analysis of the spectra does not reveal the existence of a second lifetime component. In the literature on other Al-alloys, it is also usually assumed that most positrons are trapped by vacancies due to their high concentration and that the bulk lifetime component plays a minor role [16]. Therefore, this aspect is not entirely clear.

During NSA after AA, the lifetime increases again and reaches a value of 0.213 after ≈500 min. A slight indication for a decrease after 1000 min is observed. To explain such secondary ageing it is argued that after short AA the residual solute supersaturation is still high enough to drive room temperature diffusion. According to this argument, the observed changes of the average positron lifetime during secondary ageing are due to solute redistribution within the matrix or from the matrix to the pre-existing clusters. Commonly, the re-increase of the lifetime during secondary ageing in Mg-containing alloys is attributed to Mg diffusing to the emerging clusters and further modifying their electron density. In Al-Cu(Mg) alloys it has been shown that the increase during secondary ageing [15] is no longer observed when there is no Mg in the alloy [17], which convincingly underlines the crucial role of Mg. Similar effects have been observed by a number of other authors, e.g. for 6061 alloys [3]. If we follow this argument, the decrease of lifetime during AA as during simple NA, see Figure 5, could be attributed to precipitation of predominantly Si into clusters or small zones possibly in conjunction with vacancies, while the re-increase of positron lifetime during NSA is due to diffusive processes involving Mg.

NPA prior to AA has a big influence on the secondary ageing behaviour. Even a short pre-aging of just 5 min largely slows down the lifetime increase and reduces the final lifetime reached. 10 min of NPA are sufficient to prevent any lifetime change. In other words, within the first 10 min of NPA, clustering processes occur that block the ability of the alloy to retain a supersaturation of Mg after AA that then drives secondary ageing. Possibly, during these 10 min of NPA, nuclei are formed that bind a large part of the solute during the ensuing short (1 min) AA treatment. This lifetime change during NSA is given in Fig. 5 as a function of NPA and correlates it to the measures for the negative effect. Figure 6(b) demonstrates that the effect that suppresses the lifetime change during NA is extremely temperature sensitive. NPA at 0°C for 40 min has about the same effect as 5 min at 18°C. NPA for 140 min at 0°C is sufficient to stop the lifetime increase.
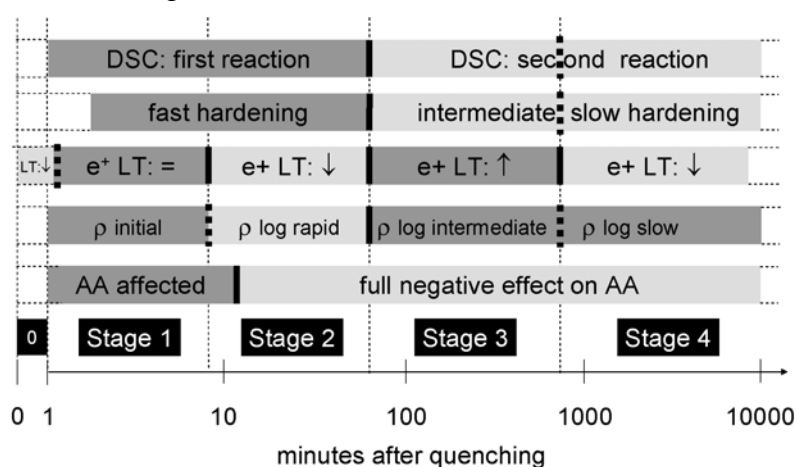
Figure 7. Schematic comparison of different characteristic lifetimes identified in the current study: e^+ LT = positron lifetime and the direction of change is indicated, ρ is electrical resistivity, 'AA affected' is range where negative effect of NPA on AA develops, in the range after the negative effect is fully established. Short vertical bars indicate transitions between stages that can be clearly identified experimentally, dotted bars indicate transitions that appear less clear or are theoretical. Horizontal dotted lines mark time domains in which no data is available.

5. Conclusions

We have shown by various methods that during NA many of the observed changes of a specific property occur at similar times. Although the exact physical origin of all these phenomena is not known with certainty, there is good reason to believe that the coincidence observed is not accidental but reflects different stages of precipitation. Figure 7 summarises the different stages, namely,

Stage 0 can be detected only indirectly. After quenching, vacancies are freely diffusing in the alloy before they get bound by a solute atom and form solute-vacancy complexes, most likely already during quenching. The evidence for this stage is that the positron lifetime in both the alloys 2–3 min after quenching is about 0.015–0.02 ns lower than that for free vacancies in Al (≈0.250 ns).

Stage 1 is only observed in alloy F and lasts until 7–10 min after quenching (at 'room temperature', longer at lower temperatures [12]). The positron lifetime is nearly constant and starts to decrease only at the transition to stage 2. Moreover, 10 min of NA lead to such a degree of clustering that during secondary ageing after 1 min of AA no more lifetime changes take place. Third, during this period, a different rate of the increase of electrical resistivity might be discernable in the in-situ measurements. Finally, the negative effect on hardness response during AA is largely established during this period. Microscopically, the formation of small Si-rich aggregates not entirely surrounding the vacancies attached to them and not closely packed seems possible. Such clustering would not have a big impact on the positron lifetime but provide nuclei for the next stage.

Stage 2: in this stage the positron lifetime during NA decreases and reaches a minimum after about 60 min (80 min) for alloy F (H). After about the same time, both the hardness and resistivity increase

in alloy F start levelling off. Finally, DSC shows that a first exothermic reaction is completed after about 60 min. Following the arguments given in the literature [10], in this stage the vacancies would be increasingly trapped and immobilised in silicon-rich clusters that become denser and therefore give rise to a reduced lifetime of the positrons.

Stage 3: the positron lifetime during NA starts increasing again in both the alloys. Slower resistivity increase, slower rate of hardening and the second cluster reaction detected in the thermal signal proceed after about the same time (>50-85 min). The diffusion of magnesium within the solid solution that is more sluggish than that of silicon now gains importance and leads to the formation of co-clusters of both Si and Mg.

Stage 4: the positron lifetime starts to decrease again (>800 min), approaching the equilibrium value very slowly. For alloy F, hardness and resistivity show a slowing of rate at 800 – 1500 min during the change from stage 3 to 4 and the area of the third peak in the DSC curve exhibits a kink. It remains to be confirmed whether these is really a defined transitions. One possible mechanism could be progressing ordering within the cluster associated with a migration of vacancies out of the clusters into the solid solution and to sinks where they annihilate.

In summary, ageing processes in aluminium 6000 alloys have been investigated by many researchers but still some fundamental questions remain unsolved. Although many methods have been applied to these alloys, comparability is difficult since each group has used different alloys in terms of Mg-Si content, alloy purity or content in further elements and also alloy processing conditions. Further investigations in the future should include more studies of the role of Mg and an attempt to measure the Doppler broadening of the positron annihilation radiation during ageing which could provide the additional local chemical information needed.

References

[1] M. Murayama and K. Hono, Acta Mater. 47 (1999) 1537-1548.

[2] A. Serizawa, S. Hirosawa and T. Sato, Met. Mater. Trans. 39A (2008) 243-251.

[3] J. Buha, P. R. Munroe, R. N. Lumley, A. G. Crosky and A. J. Hill, in Proc. 9th Int. Conf. Aluminium Alloys (Ed. by: J. F. Nie, A. J. Morton and B. C. Muddle), Institute of Materials Engineering Australasia Ltd. 2004, 1028-1033.

[4] B. Klobes, T. E. M. Staab, M. Haaks, K. Maier and I. Wieler, Phys. Stat. Sol. (RRL) 2 (2008) 224-226.

[5] H. Seyedrezai, D. Grebennikov, P. Mascher and H. S. Zurob, Mater. Sci. Eng. A525 (2009) 186-191.

[6] A. K. Gupta and D. J. Lloyd, Met. Mater. Trans. 30A (1999) 879-884.

[7] J. Røyset, T. Stene, J. A. Sæter and O. Reiso, Mat. Sci. Forum. 519-521 (2006) 239-244.

[8] A. Ried, P. Schwellinger and H. Bichsel, Aluminium 53 (1977) 595-599.

[9] H. Suzuki, M. Kanno and G. Itoh, Aluminium 67 (1981) 628-629.

[10] S. Esmaeli, W. J. Poole and D. J. Lloyd, Mater. Sci. Forum 331-337 (2000) 995-1000.

[11] C. S. T. Chang and J. Banhart, Met. Mater. Trans B (submitted, 2010).

[12] J. Banhart, M. D. H. Lay, C. S. T. Chang and A. J. Hill, eprint: http://arxiv.org/abs/1006.4778.

[13] J. Banhart, C. S. T. Chang, Z. Liang, N. Wanderka, M. D. H. Lay and A. J. Hill, Adv. Eng. Mater., in print (2010) doi: 10.1002/adem.201000041.

[14] P. Brenner and H. Kostron, Z. Metallkde. 31 (1939) 89-97.

[15] A. Somoza, A. Dupasquier, I. J. Polmear, P. Folegati and R. Ferragut, Phys. Rev. B61 (2000) 14454-14463.

[16] A. Dupasquier, G. Kögel and A. Somoza, Acta Mater. 52 (2004) 4707-4726.

[17] R. Ferragut, G. Ferro and M. Biasini, in Proc. 9th Int. Conf. Aluminium Alloys (Ed. by: J. F. Nie, A. J. Morton and B. C. Muddle), Institute of Materials Engineering Australasia Ltd. 2004, 1022-1027.